NUMERICAL SIMULATION OF CONCRETE FAILURE IN PULL-OUT EXPERIMENTS

P. Pivonka, R. Lackner, and H. A. Mang

Institute for Strength of Materials
Vienna University of Technology, Vienna, Austria

ABSTRACT

This paper deals with the application of a 3D-constitutive model for concrete to simulations of pull-out experiments [1]. This material model is formulated within the framework of multi-surface plasticity. It consists of three Rankine yield surfaces for the simulation of cracking and a Drucker-Prager yield surface for the description of compressive failure of concrete. The Drucker-Prager surface is reformulated in order to account for the influence of confinement on the compressive strength and the ductility of concrete.
The predictive capability of the model is demonstrated by means of a finite element (FE) analysis of a pull-out test [1]. The influence of confinement on the peak load and the failure mode is investigated.

KEYWORDS

multi-surface plasticity, concrete, confinement, pull-out, ultimate load, failure mode

INTRODUCTION

The use of numerical tools such as the FEM allows simulation of real-life structures characterized by complex geometric properties and loading conditions. As regards the simulation of concrete structures, sophisticated material models are required in order to provide an appropriate description of the mechanical behavior of concrete. Such material models should account for crack opening in the case of tensile loading, crushing in the case of compressive loading, and compaction of concrete when subjected to hydrostatic pressure.

In the context of plasticity theory, failure may be described either by one failure criterion (single-surface plasticity) or by a combination of several failure criteria (multi-surface plasticity). As regards multi-surface plasticity, each failure criterion is used to describe a certain mode of material failure. For the simulation of cracking, the Rankine criterion gives the best results. In the compressive loading regime, the Drucker-Prager surface is commonly employed (see, e.g., [5][9]). The compaction of concrete may be considered by means of an additional cap (see, e.g., [7]).

In this paper a multi-surface plasticity model consisting of the Drucker-Prager criterion and the Rankine criterion is considered. As regards the Drucker-Prager criterion, a reformulation is proposed in order to extend its range of applicability. The influence of this reformulation on the numerical results is demonstrated by means of a FE analysis of a pull-out test.

In the following section, the material model is briefly presented and the proposed modification of the Drucker-Prager criterion is described. However, the main part of the paper is devoted to the numerical analysis of a pull-out test.

3D PLASTICITY MODEL FOR PLAIN CONCRETE

Concrete is a composite material, made of cement, aggregates, and water. In continuum mechanics, however, concrete is treated as homogeneous material. The respective scale of observation is referred to as macro-level. Stress-strain relations formulated at the macro-level relate macro-stresses to macro-strains. However, the mechanical behavior observed at the macro-level is associated with phenomena occurring at the micro-level of the material. E.g., inelastic macro-strains arise from micro-cracking of hydrates. For the description of phenomena at the micro-level, so-called internal variables $\boldsymbol{\alpha}$ are introduced in the material model. They are used to describe the microstructural change of the material. The energetically conjugated thermodynamic quantities are the hardening/softening forces $\mathbf{q}$. They are related to the internal variables via the state equation $\mathbf{q} = \mathbf{q}(\boldsymbol{\alpha})$. The hardening forces represent the actual strength of the material, defining the space of admissible stress states, $\mathbf{C}_E$:

$$\boldsymbol{\sigma} \in \mathbf{C}_E \quad \Leftrightarrow \quad f_k = f_k(\boldsymbol{\sigma}, \mathbf{q}(\boldsymbol{\alpha})) \leq 0 \quad \forall \quad k \in [1,2,...,N] \tag{1}$$

where f_k denotes the k-th yield function. In definition (1), the general case of multi-surface plasticity is considered. N denotes the number of employed yield functions.

The internal variables and the respective deformations related to plastic material response are obtained by means of evolution equations, reading

$$\dot{\boldsymbol{\alpha}} = \sum_{k \in J_{act}} \dot{\gamma}_k \frac{\partial H_k}{\partial \mathbf{q}}, \qquad \dot{\boldsymbol{\varepsilon}}^p = \sum_{k \in J_{act}} \dot{\gamma}_k \frac{\partial Q_k}{\partial \boldsymbol{\sigma}}, \tag{2}$$

where γ_k denotes the plastic multiplier of the k-th yield function. H_k and Q_k are potentials which, in general, depend on $\boldsymbol{\sigma}$ and $\mathbf{q}$.

The material model considered in this paper is formulated within the framework of multi-surface plasticity theory. It consists of four yield surfaces ($N = 4$): a Drucker-Prager (DP) yield surface for the description of concrete when subjected to compressive loading and three Rankine (RK) surfaces for the description of tensile failure. In the principal stress space, the failure criteria read

$$f_{DP}(\boldsymbol{\sigma}, q_{DP}) = \sqrt{J_2} - \kappa_{DP} I_1 - \frac{\bar{q}_{DP}}{\beta_{DP}}, \text{ with } \quad \bar{q}_{DP} = f_{cy} - q_{DP}, \tag{3}$$

and

$$f_{RK,A}(\sigma_A, q_{RK}) = \sigma_A - \bar{q}_{RK}, \text{ with } \quad \bar{q}_{RK} = f_{tu} - q_{RK}, \tag{4}$$

where the subscript A ($A = 1,2,3$) refers to one of the three principal axes. f_{tu} is the tensile strength and f_{cy} represents the elastic limit of concrete under uniaxial compressive loading. κ_{DP} and β_{DP} are constant material parameters.

For the description of microstructural changes of concrete, two internal variables are employed: α_{RK} and α_{DP}. They are computed by means of associated hardening/softening laws, i.e., $H_{RK,A} = f_{RK,A}$ and $H_{DP} = f_{DP}$, reading

$$\dot{\alpha}_{RK} = \sum_{A=1}^{3} \gamma_{RK,A} \frac{\partial f_{RK,A}}{\partial q_{RK}}, \quad \dot{\alpha}_{DP} = \sum_{A=1}^{3} \gamma_{DP} \frac{\partial f_{DP}}{\partial q_{DP}}. \tag{5}$$

Cracking of concrete is characterized by a continuous decrease of the tensile strength $\bar{q}_{RK}$. Accordingly, an exponential softening law is chosen, reading

$$\bar{q}_{RK} = f_{tu} \exp[-\alpha_{RK} / \alpha_{RK,u}], \tag{6}$$

where $\alpha_{RK,u}$ is a calibration parameter. Under compressive loading, however, the behavior of concrete is characterized by hardening as well as softening behavior. The chosen hardening/softening curve for the compressive strength $\bar{q}_{DP}$ is depicted in Figure 1(a).

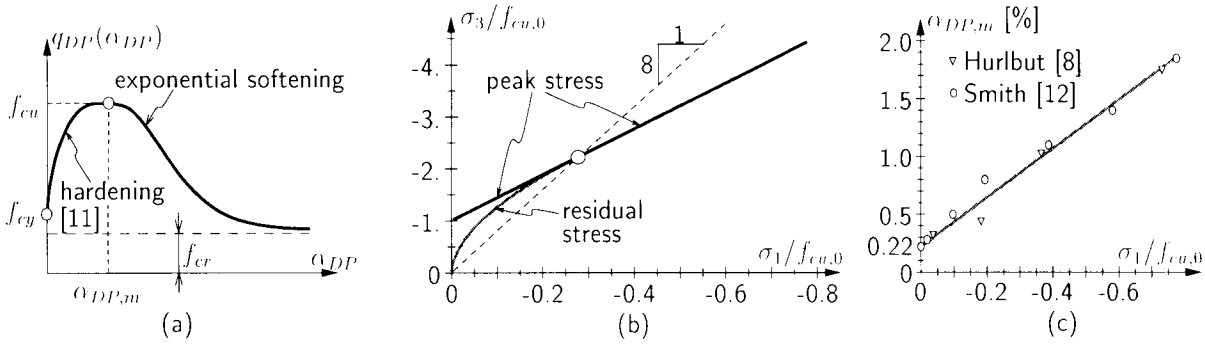

Figure 1: (a) employed hardening/softening curve for the Drucker-Prager criterion; influence of confinement on (b) the peak and residual stress (related to f_{cu} and f_{cr}) and (c) the ductility ($\alpha_{DP,m}$). The level of confinement is represented by the maximum principal stress σ_1 ($f_{cu,0}$: uniaxial compressive strength of concrete)

Commonly, the Drucker-Prager criterion is calibrated by means of uniaxial and biaxial compression tests, giving κ_{DP} and β_{DP} (see, e.g., [10]). For the application of the Drucker-Prager criterion to structures mainly experiencing biaxial stress states, this mode of calibration is appropriate. For confined stress states, however, large deviations between experimental data and numerical results were reported in [11]. Experimental data indicate an influence of confinement on both the compressive strength, described by the ultimate and the residual strengths, f_{cu} and f_{cr}, and the ductility [12]. The proposed modification of the Drucker-Prager criterion accounts for this influence by relating f_{cu}, f_{cr}, and $\alpha_{DP,m}$ to the actual level of confinement. Confinement is represented by the major principal stress σ_1, with $\sigma_1 \geq \sigma_2 \geq \sigma_3$, yielding $f_{cu} = f_{cu}(\sigma_3(\sigma_1))$, $f_{cr} = f_{cr}(\sigma_3(\sigma_1))$, and $\alpha_{DP,m} = \alpha_{DP,m}(\sigma_1)$ (see Figure 1(b) and (c)). f_{cu} and

f_{cr} are computed by means of the Drucker-Prager criterion, $f_{DP}=0$, using the stress state $\boldsymbol{\sigma}^T=[\sigma_1,\sigma_1,\sigma_3(\sigma_1)]$ (for details, see [11]).

FAILURE ANALYSIS OF PULL-OUT TEST

The focus of the present paper is on the influence of the underlying model formulation on numerical results obtained from failure analyses of anchor bolts in concrete, referred to as pull-out test. For this purpose, analyses on the basis of the material model described in the previous section were performed. The influence of confinement on the peak load and on the failure mode is investigated.

Geometric dimensions and material properties

Figure 2 contains the experimental setup of the considered pull-out test (Round-robin test [1]). It shows the geometric dimensions as well as the support conditions of the specimen. Further, the material properties of concrete and steel are given.

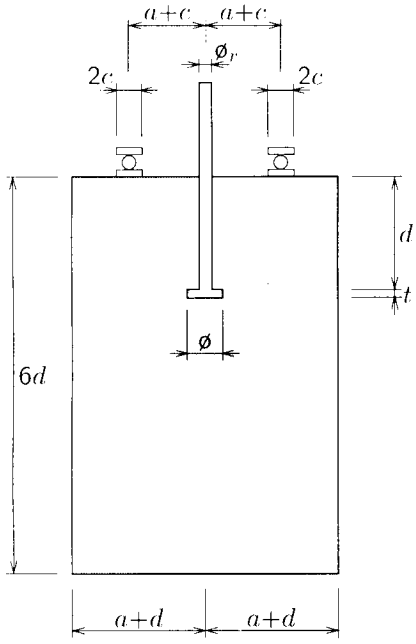

dimensions:

d=150 mm a=150 mm

t=15 mm c=22.5 mm

ø=45 mm $ø_r$=24 mm

concrete:

Young's modulus: E_c=30000 N/mm^2

Poisson's ratio: ν_c=0.2

uniaxial compressive strength: f_{cu}=40 N/mm^2

uniaxial tensile strength: f_{tu}=3 N/mm^2

fracture energy: G_f^I=0.1 Nmm/mm^2

fracture energy: G_f^{II}=50G_f^I

steel:

Young's modulus: E_s=210000 N/mm^2

Poisson's ratio: ν_s=0.3

Figure 2: Pull-out analysis: geometric dimensions and material properties

Numerical analysis

In the numerical analysis, the material behavior of the steel bolt is assumed to be linear elastic. For the description of concrete, the previously described material model is used.

Because of symmetry of the geometric properties and the loading conditions, the problem is solved by means of axisymmetric analyses. Figure 4 shows the employed FE mesh consisting of 677 four-node finite elements. As regards the mechanical model of the anchor bolt, only the anchor head is discretized. At the contact line between the anchor head and the concrete, no slip is considered. The analyses is performed displacement-driven. The displacement at the nodes of the anchor head located at the axis of symmetry is prescribed (see Figure 3).

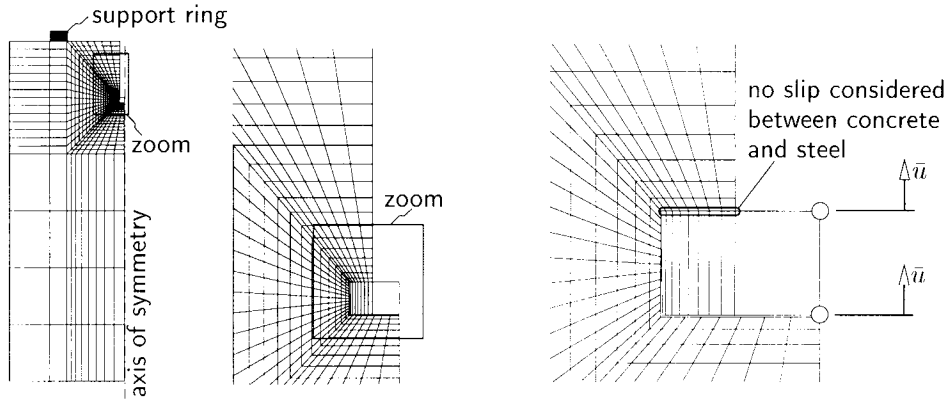

Figure 3: Pull-out analysis: FE discretization

Softening functions appearing in the formulations of the model were calibrated according to the fictitious crack concept [6]. The application of the fictitious crack concept to the simulation of radial cracks in axisymmetric analyses requires the input of the expected number of radial cracks. In the present analyses, four radial cracks are assumed to develop.

Figure 4 contains the obtained load-displacement curves. The peak load obtained from the Drucker-Prager criterion characterized by consideration of confinement (*modified* model) was found to be 340 kN. Neglection of the influence of confinement within the Drucker-Prager criterion (*original* model), i.e., setting $f_{cu} = const.$, $f_{cr} = const.$, and $\alpha_{DP,m} = 0.0022$, led to a reduction of the peak load by 47% (see Figure 4(a)).

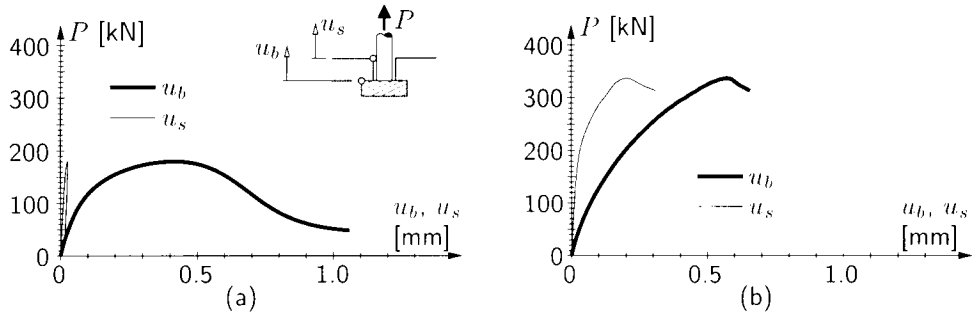

Figure 4: Pull-out analysis: load-displacement curves obtained from multi-surface model with (a) *original* and (b) *modified* Drucker-Prager criterion

The difference between the displacement at the anchor head and the concrete surface, $u_b - u_s$, is an indicator for compressive failure of concrete over the anchor head. An almost constant evolution of $u_b - u_s$ indicates a rigid body motion in consequence of formation of a cone-like failure mode (see, e.g., Figure 7(a)). Small values of u_s together with continuously increasing values of $u_b - u_s$ indicate local failure of concrete over the anchor head. This failure mode was obtained from the analysis based on the *original* model (see Figure 4(a)). The underestimation of compressive strength and ductility by neglecting the influence of confinement resulted in compressive failure of concrete over the anchor head. The respective $P - u_b$ curve shows similar characteristics as the underlying hardening/softening curve used for the Drucker-Prager model (see Figure 1(a)). Moreover, failure of concrete over the anchor head resulted in an unloading of the remaining part of the structure. This is reflected by the decrease of u_s in the post-peak regime. Consideration of confinement by the *modified* model led to an increase of the compressive strength over the anchor head. The almost constant evolution of $u_b - u_s$ in the post-peak regime (Figure 4(b)) indicates the development of a cone-like failure mode (see Figure 7(a)).

The distribution of α_{DP} is given in Figure 5 for both analyses at the respective peak loads. The compressive failure over the anchor head obtained from the *original* model is reflected by softening material behavior (see Figure 5(a)). Softening is characterized by $\alpha_{DP} > \alpha_{DP,m} = 0.0022$. On the other hand, confinement considered in the analysis based on the *modified* model resulted in an increase of $\alpha_{DP,m}$ over the anchor head (see Figure 5(c)). The distribution of α_{DP} is shown in Figure 5(b). The values of α_{DP} are lower than the respective values of $\alpha_{DP,m}$ indicating that the compressive strength in this area has not reached the ultimate strength f_{cu} (hardening regime).

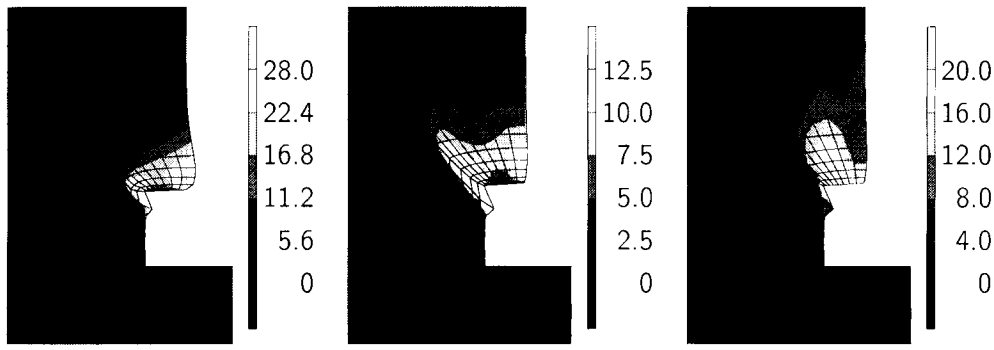

Figure 5: Pull-out analysis: distribution of, α_{DP} at peak load obtained from multi-surface model with (a) *original* and (b) *modified* Drucker-Prager criterion; (c) distribution of $\alpha_{DP,m}$ at peak load obtained from multi-surface model with *modified* Drucker-Prager criterion (10-fold magnification of displacements)

The strong influence of confinement on the obtained numerical results is a consequence of large compressive stresses over the anchor head. Recall, the major principal stress is used as a measure for confinement. If the major principal stress is positive, no confinement is considered. Figure 6 shows the distribution of the two principal stresses in the $r-z$ plane, denoted as $\sigma_{\min}$ and $\sigma_{\max}$, and the circumferential stress σ_{circ} at peak load obtained from the analysis based on the *modified* model. Over the anchor head, negative stresses are observed for all three principal stresses. Hence, $\sigma_1 < 0$, resulting in an increase of the compressive strength and the ductility (see Figure 1(b) and (c)).

The distribution of the minimum in-plane principal stress $\sigma_{\min}$ (see Figure 6(a)) provides insights into the load-carrying behavior of the concrete specimen. The applied load at the anchor head is transferred by a compressive strut from the confined area over the anchor head to the support ring (see [2][3] for similar results). The respective maximum principal stress in this strut resulted in the development of a circumferential crack. This crack started to open at the anchor head propagating towards the support ring finally causing cone-shaped failure of the specimen. The crack pattern obtained at peak load on the basis of the *modified* model is shown in Figure 7(a) by means of the distribution of the maximum plastic strain in the $r-z$ plane, $\varepsilon^p_{\max}$. In addition to the circumferential crack, radial cracks developed, starting from the corner at the concrete surface and propagating in the interior of the concrete block. Recall, four radial cracks were assumed to open in the context of the employed fictitious crack concept. In Figure 7(b), the location of these radial cracks is shown by means of the respective circumferential plastic strain, ε^p_{circ}.

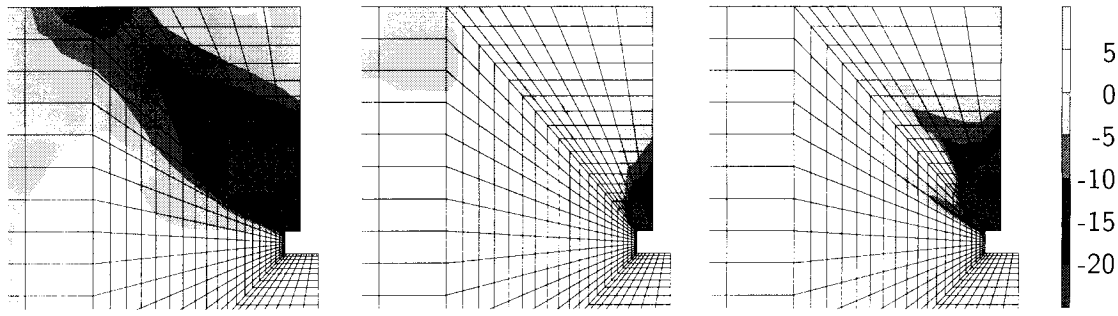

(a) σ_{min} (b) σ_{max} (c) σ_{circ}

Figure 6: Pull-out analysis: distribution of principal stresses in the $r-z$ plane, $\sigma_{\min}$ and $\sigma_{\max}$, and the stress component in the circumferential direction, σ_{circ}, at peak load obtained from multi-surface model with *modified* Drucker-Prager criterion (in [N/mm^2])

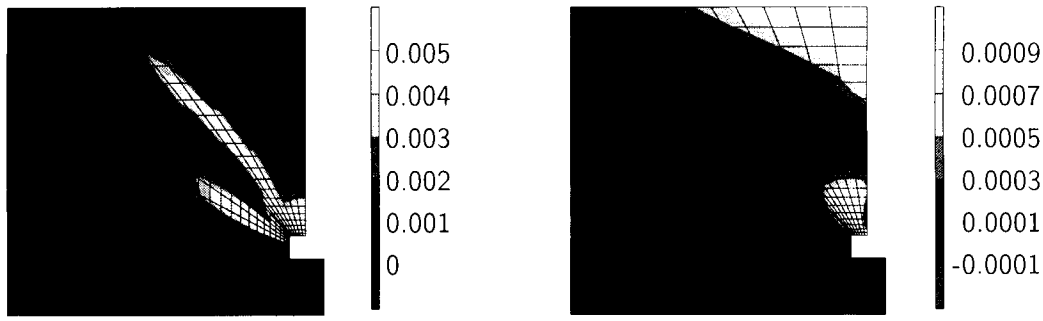

(a) ε^p_{max} (b) ε^p_{circ}

Figure 7: Pull-out analysis: distribution of the maximum plastic strain in the $r-z$ plane, $\varepsilon^p_{\max}$ and of the circumferential plastic strain ε^p_{circ} at peak load obtained from multi-surface model with *modified* Drucker-Prager criterion

CONCLUSIONS

In this paper, structural failure of anchor bolts placed in concrete was investigated. For this purpose a multi-surface plasticity model for plain concrete was used. This model was originally proposed by Meschke [9] (it is referred to as *original* model). The Drucker-Prager model was reformulated in order to account for the influence of confinement. The reformulated model is referred to as *modified* model. From the numerical simulations, the following conclusions concerning the structural response of the concrete specimen can be drawn:

- the concrete located between the anchor head and the support ring is subjected to strong non-uniform triaxal stress states, characterized by
  - hydrostatic pressure over the anchor head,
  - a compressive strut from the anchor head to the support ring, and
  - circumferential cracking caused by tensile loading perpendicular to this strut;
- the underlying model formulation has a crucial influence on the predicted failure mode characterized either
  - by local compressive failure over the anchor head, or

- by a cone-shaped failure surface in consequence of the development of circumferential cracks.

The cone-shaped failure surface, which presumably represents the correct failure mode, was obtained by the *modified* multi-surface model. Disregard of the influence of confinement on the material strength and ductility in the context of the *original* multi-surface model resulted in local compressive failure of concrete over the anchor head. The peak load related to this presumably incorrect failure mode was found to be significantly lower than the peak load obtained from the analyses characterized by cone-shaped failure.

REFERENCES

1. L. Elfgren. Fracture mechanics of concrete structures. Technical report, RILEM, Technical Committee 90, 1990.
2. G. Etse. *T*heoretische und numerische Untersuchung zum diffusen und lokalisierten Versagen in Beton. PhD thesis, Universität Karlsruhe, Karlsruhe, Germany, 1992. In German.
3. G. Etse. Finite element analysis of failure response behavior of anchor bolts in concrete. *Int. Journal of Nuclear Engineering and Design*, 179:245–252, 1998.
4. G. Etse and K. Willam. Fracture energy formulation for inelastic behavior of plain concrete. *Journal of Engineering Mechanics (ASCE)*, 120:1983–2011, 1994.
5. Ch. Hellmich, F.-J. Ulm, and H. A. Mang. Multisurface chemoplasticity I: Material model for shotcrete. *Journal of Engineering Mechanics (ASCE)*, 125(6):692–701, 1999.
6. A. Hillerborg, M. Modeer, and P. E. Petersson. Analysis of crack formation and crack growth in concrete by means of fracture mechanics and finite elements. *Cement and Concrete Research*, 6:773–782, 1976.
7. G. Hofstetter, J. C. Simo, and R. L. Taylor. A modified cap model: closest point solution algorithms. *Computers & Structures*, 46(2):203–214, 1993.
8. B. Hurlbut. Experimental and computational investigation of strain-softening in concrete. Master's thesis, University of Colorado, Boulder, USA, 1985.
9. G. Meschke. Consideration of aging of shotcrete in the context of a 3D viscoplastic material model. *International Journal for Numerical Methods in Engineering*, 39:3123–3143, 1996.
10. G. Meschke, R. Lackner, and H. A. Mang. An anisotropic elastoplastic-damage model for plain concrete. *International Journal for Numerical Methods in Engineering*, 42(4):703–727, 1998.
11. P. Pivonka, R. Lackner, and H. Mang. Numerical analyses of concrete subjected to triaxial compressive loading. In *CD-ROM Proceedings of the European Congress on Computational Methods in Applied Sciences and Engineering*, Barcelona, Spain, 2000.
12. S. Smith. On fundamental aspects of concrete behavior. Master's thesis, University of Colorado, Boulder, USA, 1987.